

FEATURES

- FET input amplifier**
- 1 pA input bias current**
- Low cost**
- High speed: 145 MHz, -3 dB bandwidth (G = +1)**
- 180 V/μs slew rate (G = +2)**
- Low noise**
 - 7 nV/√Hz (f = 10 kHz)
 - 0.6 fA/√Hz (f = 10 kHz)
- Wide supply voltage range: 5 V to 24 V**
- Single-supply and rail-to-rail output**
- Low offset voltage 1.5 mV max**
- High common-mode rejection ratio: -100 dB**
- Excellent distortion specifications**
- SFDR -88 dB @ 1 MHz**
- Low power: 6.4 mA/amplifier typical supply current**
- No phase reversal**
- Small packaging: SOIC-8, SOT-23-5, and MSOP**

GENERAL DESCRIPTION

The AD8065/AD8066¹ FastFET amplifiers are voltage feedback amplifiers with FET inputs offering high performance and ease of use. The AD8065 is a single amplifier, and the AD8066 is a dual amplifier. These amplifiers are developed in the Analog Devices, Inc. proprietary XFCB process and allow exceptionally low noise operation (7.0 nV/√Hz and 0.6 fA/√Hz) as well as very high input impedance.

With a wide supply voltage range from 5 V to 24 V, the ability to operate on single supplies, and a bandwidth of 145 MHz, the AD8065/AD8066 are designed to work in a variety of applications. For added versatility, the amplifiers also contain rail-to-rail outputs.

Despite the low cost, the amplifiers provide excellent overall performance. The differential gain and phase errors of 0.02% and 0.02°, respectively, along with 0.1 dB flatness out to 7 MHz, make these amplifiers ideal for video applications. Additionally, they offer a high slew rate of 180 V/μs, excellent distortion (SFDR of -88 dB @ 1 MHz), extremely high common-mode rejection of -100 dB, and a low input offset voltage of 1.5 mV maximum under warmed up conditions. The AD8065/AD8066

¹Protected by U. S. Patent No. 6,262,633.

Rev. E

Information furnished by Analog Devices is believed to be accurate and reliable. However, no responsibility is assumed by Analog Devices for its use, nor for any infringements of patents or other rights of third parties that may result from its use. Specifications subject to change without notice. No license is granted by implication or otherwise under any patent or patent rights of Analog Devices. Trademarks and registered trademarks are the property of their respective owners.

APPLICATIONS

- Instrumentation
- Photodiode preamps
- Filters
- A/D drivers
- Level shifting
- Buffering

CONNECTION DIAGRAMS

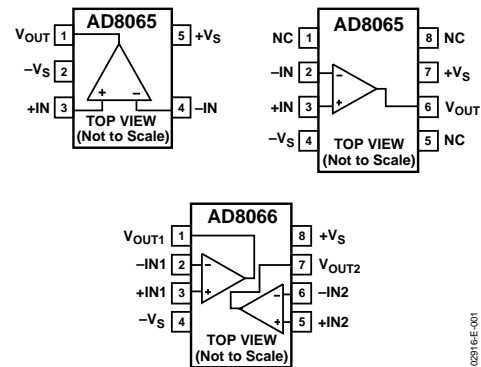


Figure 1.

operate using only a 6.4 mA/amplifier typical supply current and are capable of delivering up to 30 mA of load current.

The AD8065/AD8066 are high performance, high speed, FET input amplifiers available in small packages: SOIC-8, MSOP-8, and SOT-23-5. They are rated to work over the industrial temperature range of -40°C to +85°C.

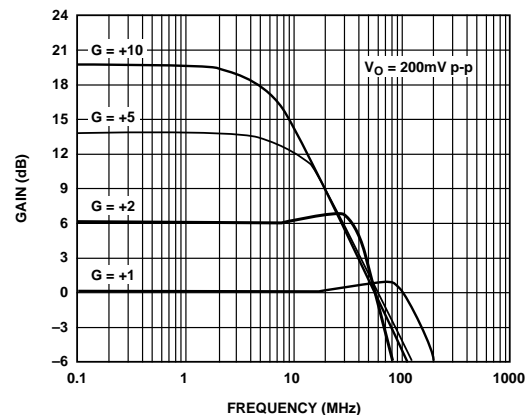


Figure 2. Small Signal Frequency Response

TABLE OF CONTENTS

Specifications..... 3

Absolute Maximum Ratings..... 6

 ESD Caution..... 6

 Maximum Power Dissipation 7

 Output Short Circuit..... 7

Typical Performance Characteristics 8

Test Circuits..... 15

Theory of Operation 18

 Closed-Loop Frequency Response..... 18

 Noninverting Closed-Loop Frequency Response 18

 Inverting Closed-Loop Frequency Response 18

 Wideband Operation 19

 Input Protection..... 19

 Thermal Considerations..... 20

 Input and Output Overload Behavior..... 20

Layout, Grounding, and Bypassing Considerations..... 21

 Power Supply Bypassing 21

 Grounding 21

 Leakage Currents..... 22

 Input Capacitance..... 22

 Output Capacitance 22

 Input-to-Output Coupling..... 23

 Wideband Photodiode Preamp 23

 High Speed JFET Input Instrumentation Amplifier..... 24

 Video Buffer 24

Outline Dimensions 25

 Ordering Guide..... 26

REVISION HISTORY

2/04—Data Sheet Changed from Rev. D to Rev. E.

Updated Format..... Universal

Updated Figure 56 21

Updated Outline Dimensions 25

Updated Ordering Guide..... 26

11/03—Data Sheet changed from Rev. C to Rev. D.

Changes to Features 1

Changes to Connection Diagrams 1

Updated Ordering Guide..... 5

Updated Outline Dimensions 22

4/03—Data Sheet changed from Rev. B to Rev. C.

Added SOIC-8 (R) for the AD8065..... 4

2/03—Data Sheet changed from Rev. A to Rev. B.

Changes to Absolute Maximum Ratings..... 4

Changes to Test Circuit 10 14

Changes to Test Circuit 11 15

Changes to Noninverting Closed-Loop Frequency Response 16

Changes to Inverting Closed-Loop Frequency Response 16

Updated Figure 6 18

Changes to Figure 7..... 19

Changes to Figures 10..... 21

Changes to Figure 11..... 22

Changes to High Speed JFET Instrumentation Amplifier 22

Changes to Video Buffer..... 22

8/02—Data Sheet changed from Rev. 0 to Rev. A.

Added AD8066 Universal

Added SOIC-8 (R) and MSOP-8 (RM) 1

Edits to General Description 1

Edits to Specifications..... 2

New Figure 2 5

Changes to Ordering Guide 5

Edits to TPCs 18, 25, and 28..... 8

New TPC 36 11

Added Test Circuits 10 and 11 14

MSOP (RM-8) added..... 23

SPECIFICATIONS

@ $T_A = 25^\circ\text{C}$, $V_S = \pm 5\text{ V}$, $R_L = 1\text{ k}\Omega$, unless otherwise noted.

Table 1.

Parameter	Conditions	Min	Typ	Max	Unit
DYNAMIC PERFORMANCE					
–3 dB Bandwidth	$G = +1$, $V_O = 0.2\text{ V p-p}$ (AD8065)	100	145		MHz
	$G = +1$, $V_O = 0.2\text{ V p-p}$ (AD8066)	100	120		MHz
Bandwidth for 0.1 dB Flatness	$G = +2$, $V_O = 0.2\text{ V p-p}$		50		MHz
	$G = +2$, $V_O = 2\text{ V p-p}$		42		MHz
Input Overdrive Recovery Time	$G = +2$, $V_O = 0.2\text{ V p-p}$		7		MHz
Output Recovery Time	$G = +1$, $-5.5\text{ V to }+5.5\text{ V}$		175		ns
Slew Rate	$G = -1$, $-5.5\text{ V to }+5.5\text{ V}$		170		ns
Settling Time to 0.1%	$G = +2$, $V_O = 4\text{ V Step}$	130	180		V/ μs
	$G = +2$, $V_O = 2\text{ V Step}$		55		ns
	$G = +2$, $V_O = 8\text{ V Step}$		205		ns
NOISE/HARMONIC PERFORMANCE					
SFDR	$f_C = 1\text{ MHz}$, $G = +2$, $V_O = 2\text{ V p-p}$		–88		dBc
	$f_C = 5\text{ MHz}$, $G = +2$, $V_O = 2\text{ V p-p}$		–67		dBc
	$f_C = 1\text{ MHz}$, $G = +2$, $V_O = 8\text{ V p-p}$		–73		dBc
Third-Order Intercept	$f_C = 10\text{ MHz}$, $R_L = 100\ \Omega$		24		dBm
Input Voltage Noise	$f = 10\text{ kHz}$		7		nV/ $\sqrt{\text{Hz}}$
Input Current Noise	$f = 10\text{ kHz}$		0.6		fA/ $\sqrt{\text{Hz}}$
Differential Gain Error	NTSC, $G = +2$, $R_L = 150\ \Omega$		0.02		%
Differential Phase Error	NTSC, $G = +2$, $R_L = 150\ \Omega$		0.02		Degree
DC PERFORMANCE					
Input Offset Voltage	$V_{CM} = 0\text{ V}$, SOIC Package		0.4	1.5	mV
Input Offset Voltage Drift			1	17	$\mu\text{V}/^\circ\text{C}$
Input Bias Current	SOIC Package		2	6	pA
	T_{MIN} to T_{MAX}		25		pA
Input Offset Current			1	10	pA
	T_{MIN} to T_{MAX}		1		pA
Open-Loop Gain	$V_O = \pm 3\text{ V}$, $R_L = 1\text{ k}\Omega$	100	113		dB
INPUT CHARACTERISTICS					
Common-Mode Input Impedance			1000 2.1		$\text{G}\Omega$ pF
Differential Input Impedance			1000 4.5		$\text{G}\Omega$ pF
Input Common-Mode Voltage Range					
FET Input Range		–5 to +1.7	–5.0 to +2.4		V
Usable Range	See the Theory of Operation section		–5.0 to +5.0		V
Common-Mode Rejection Ratio	$V_{CM} = -1\text{ V to }+1\text{ V}$	–85	–100		dB
	$V_{CM} = -1\text{ V to }+1\text{ V}$ (SOT-23)	–82	–91		dB
OUTPUT CHARACTERISTICS					
Output Voltage Swing	$R_L = 1\text{ k}\Omega$	–4.88 to +4.90	–4.94 to +4.95		V
	$R_L = 150\ \Omega$		–4.8 to +4.7		V
Output Current	$V_O = 9\text{ V p-p}$, SFDR $\geq -60\text{ dBc}$, $f = 500\text{ kHz}$		35		mA
Short-Circuit Current			90		mA
Capacitive Load Drive	30% Overshoot $G = +1$		20		pF
POWER SUPPLY					
Operating Range		5		24	V
Quiescent Current per Amplifier			6.4	7.2	mA
Power Supply Rejection Ratio	$\pm\text{PSRR}$	–85	–100		dB

AD8065/AD8066

@ $T_A = 25^\circ\text{C}$, $V_S = \pm 12\text{ V}$, $R_L = 1\text{ k}\Omega$, unless otherwise noted.

Table 2.

Parameter	Conditions	Min	Typ	Max	Unit
DYNAMIC PERFORMANCE					
–3 dB Bandwidth	$G = +1$, $V_O = 0.2\text{ V p-p}$ (AD8065)	100	145		MHz
	$G = +1$, $V_O = 0.2\text{ V p-p}$ (AD8066)	100	115		MHz
Bandwidth for 0.1 dB Flatness	$G = +2$, $V_O = 0.2\text{ V p-p}$		50		MHz
	$G = +2$, $V_O = 2\text{ V p-p}$		40		MHz
Input Overdrive Recovery	$G = +1$, $-12.5\text{ V to }+12.5\text{ V}$		175		ns
Output Overdrive Recovery	$G = -1$, $-12.5\text{ V to }+12.5\text{ V}$		170		ns
Slew Rate	$G = +2$, $V_O = 4\text{ V Step}$	130	180		V/ μs
Settling Time to 0.1%	$G = +2$, $V_O = 2\text{ V Step}$		55		ns
	$G = +2$, $V_O = 10\text{ V Step}$		250		ns
NOISE/HARMONIC PERFORMANCE					
SFDR	$f_C = 1\text{ MHz}$, $G = +2$, $V_O = 2\text{ V p-p}$		–100		dBc
	$f_C = 5\text{ MHz}$, $G = +2$, $V_O = 2\text{ V p-p}$		–67		dBc
	$f_C = 1\text{ MHz}$, $G = +2$, $V_O = 10\text{ V p-p}$		–85		dBc
Third-Order Intercept	$f_C = 10\text{ MHz}$, $R_L = 100\ \Omega$		24		dBm
Input Voltage Noise	$f = 10\text{ kHz}$		7		nV/ $\sqrt{\text{Hz}}$
Input Current Noise	$f = 10\text{ kHz}$		1		fA/ $\sqrt{\text{Hz}}$
Differential Gain Error	NTSC, $G = +2$, $R_L = 150\ \Omega$		0.04		%
Differential Phase Error	NTSC, $G = +2$, $R_L = 150\ \Omega$		0.03		Degree
DC PERFORMANCE					
Input Offset Voltage	$V_{CM} = 0\text{ V}$, SOIC Package		0.4	1.5	mV
Input Offset Voltage Drift			1	17	$\mu\text{V}/^\circ\text{C}$
Input Bias Current	SOIC Package		3	7	pA
	T_{MIN} to T_{MAX}		25		pA
Input Offset Current			2	10	pA
	T_{MIN} to T_{MAX}		2		pA
Open-Loop Gain	$V_O = \pm 10\text{ V}$, $R_L = 1\text{ k}\Omega$	103	114		dB
INPUT CHARACTERISTICS					
Common-Mode Input Impedance			1000 2.1		$\text{G}\Omega$ pF
Differential Input Impedance			1000 4.5		$\text{G}\Omega$ pF
Input Common-Mode Voltage Range					
FET Input Range		–12 to +8.5	–12.0 to +9.5		V
Usable Range	See the Theory of Operation section		–12.0 to +12.0		V
Common-Mode Rejection Ratio	$V_{CM} = -1\text{ V to }+1\text{ V}$	–85	–100		dB
	$V_{CM} = -1\text{ V to }+1\text{ V}$ (SOT-23)	–82	–91		dB
OUTPUT CHARACTERISTICS					
Output Voltage Swing	$R_L = 1\text{ k}\Omega$	–11.8 to +11.8	–11.9 to +11.9		V
	$R_L = 350\ \Omega$		–11.25 to +11.5		V
Output Current	$V_O = 22\text{ V p-p}$, SFDR $\geq -60\text{ dBc}$, $f = 500\text{ kHz}$		30		mA
Short-Circuit Current			120		mA
Capacitive Load Drive	30% Overshoot $G = +1$		25		pF
POWER SUPPLY					
Operating Range		5		24	V
Quiescent Current per Amplifier			6.6	7.4	mA
Power Supply Rejection Ratio	$\pm\text{PSRR}$	–84	–93		dB

@ $T_A = 25^\circ\text{C}$, $V_S = 5\text{ V}$, $R_L = 1\text{ k}\Omega$, unless otherwise noted.

Table 3.

Parameter	Conditions	Min	Typ	Max	Unit
DYNAMIC PERFORMANCE					
–3 dB Bandwidth	$G = +1$, $V_O = 0.2\text{ V p-p}$ (AD8065)	125	155		MHz
	$G = +1$, $V_O = 0.2\text{ V p-p}$ (AD8066)	110	130		MHz
Bandwidth for 0.1 dB Flatness	$G = +2$, $V_O = 0.2\text{ V p-p}$		50		MHz
	$G = +2$, $V_O = 2\text{ V p-p}$		43		MHz
Input Overdrive Recovery Time	$G = +1$, $-0.5\text{ V to }+5.5\text{ V}$		175		ns
Output Recovery Time	$G = -1$, $-0.5\text{ V to }+5.5\text{ V}$		170		ns
Slew Rate	$G = +2$, $V_O = 2\text{ V Step}$	105	160		V/ μs
Settling Time to 0.1%	$G = +2$, $V_O = 2\text{ V Step}$		60		ns
NOISE/HARMONIC PERFORMANCE					
SFDR	$f_C = 1\text{ MHz}$, $G = +2$, $V_O = 2\text{ V p-p}$		–65		dBc
	$f_C = 5\text{ MHz}$, $G = +2$, $V_O = 2\text{ V p-p}$		–50		dBc
Third-Order Intercept	$f_C = 10\text{ MHz}$, $R_L = 100\ \Omega$		22		dBm
Input Voltage Noise	$f = 10\text{ kHz}$		7		nV/ $\sqrt{\text{Hz}}$
Input Current Noise	$f = 10\text{ kHz}$		0.6		fA/ $\sqrt{\text{Hz}}$
Differential Gain Error	NTSC, $G = +2$, $R_L = 150\ \Omega$		0.13		%
Differential Phase Error	NTSC, $G = +2$, $R_L = 150\ \Omega$		0.16		Degree
DC PERFORMANCE					
Input Offset Voltage	$V_{CM} = 1.0\text{ V}$, SOIC Package		0.4	1.5	mV
Input Offset Voltage Drift			1	17	$\mu\text{V}/^\circ\text{C}$
Input Bias Current	SOIC Package		1	5	pA
	T_{MIN} to T_{MAX}		25		pA
Input Offset Current			1	5	pA
	T_{MIN} to T_{MAX}		1		pA
Open-Loop Gain	$V_O = 1\text{ V to }4\text{ V}$ (AD8065)	100	113		dB
	$V_O = 1\text{ V to }4\text{ V}$ (AD8066)	90	103		dB
INPUT CHARACTERISTICS					
Common-Mode Input Impedance			1000 2.1		$\text{G}\Omega$ pF
Differential Input Impedance			1000 4.5		$\text{G}\Omega$ pF
Input Common-Mode Voltage Range					
FET Input Range		0 to 1.7	0 to 2.4		V
Usable Range	See the Theory of Operation section		0 to 5.0		V
Common-Mode Rejection Ratio	$V_{CM} = 1\text{ V to }4\text{ V}$	–74	–100		dB
	$V_{CM} = 1\text{ V to }2\text{ V}$ (SOT-23)	–78	–91		dB
OUTPUT CHARACTERISTICS					
Output Voltage Swing	$R_L = 1\text{ k}\Omega$	0.1 to 4.85	0.03 to 4.95		V
	$R_L = 150\ \Omega$		0.07 to 4.83		V
Output Current	$V_O = 4\text{ V p-p}$, SFDR $\geq -60\text{ dBc}$, $f = 500\text{ kHz}$		35		mA
Short-Circuit Current			75		mA
Capacitive Load Drive	30% Overshoot $G = +1$		5		pF
POWER SUPPLY					
Operating Range		5		24	V
Quiescent Current per Amplifier		5.8	6.4	7.0	mA
Power Supply Rejection Ratio	$\pm\text{PSRR}$	–78	–100		dB

ABSOLUTE MAXIMUM RATINGS

Table 4.

Parameter	Rating
Supply Voltage	26.4 V
Power Dissipation	See Figure 3
Common-Mode Input Voltage	$V_{EE} - 0.5 \text{ V}$ to $V_{CC} + 0.5 \text{ V}$
Differential Input Voltage	1.8 V
Storage Temperature	-65°C to +125°C
Operating Temperature Range	-40°C to +85°C
Lead Temperature Range (Soldering, 10 sec)	300°C

Stresses above those listed under Absolute Maximum Ratings may cause permanent damage to the device. This is a stress rating only; functional operation of the device at these or any other conditions above those indicated in the operational section of this specification is not implied. Exposure to absolute maximum rating conditions for extended periods may affect device reliability.

ESD CAUTION

ESD (electrostatic discharge) sensitive device. Electrostatic charges as high as 4000 V readily accumulate on the human body and test equipment and can discharge without detection. Although this product features proprietary ESD protection circuitry, permanent damage may occur on devices subjected to high energy electrostatic discharges. Therefore, proper ESD precautions are recommended to avoid performance degradation or loss of functionality.



MAXIMUM POWER DISSIPATION

The maximum safe power dissipation in the AD8065/AD8066 packages is limited by the associated rise in junction temperature (T_j) on the die. The plastic encapsulating the die will locally reach the junction temperature. At approximately 150°C, which is the glass transition temperature, the plastic will change its properties. Even temporarily exceeding this temperature limit can change the stresses that the package exerts on the die, permanently shifting the parametric performance of the AD8065/AD8066. Exceeding a junction temperature of 175°C for an extended period of time can result in changes in the silicon devices, potentially causing failure.

The still-air thermal properties of the package and PCB (θ_{JA}), ambient temperature (T_A), and total power dissipated in the package (P_D) determine the junction temperature of the die. The junction temperature can be calculated as

$$T_j = T_A + (P_D \times \theta_{JA})$$

The power dissipated in the package (P_D) is the sum of the quiescent power dissipation and the power dissipated in the package due to the load drive for all outputs. The quiescent power is the voltage between the supply pins (V_S) times the quiescent current (I_S). Assuming the load (R_L) is referenced to midsupply, then the total drive power is $V_S/2 \times I_{OUT}$, some of which is dissipated in the package and some in the load ($V_{OUT} \times I_{OUT}$). The difference between the total drive power and the load power is the drive power dissipated in the package.

$$P_D = \text{Quiescent Power} + (\text{Total Drive Power} - \text{Load Power})$$

$$P_D = (V_S \times I_S) + \left(\frac{V_S}{2} \times \frac{V_{OUT}}{R_L} \right) - \frac{V_{OUT}^2}{R_L}$$

RMS output voltages should be considered. If R_L is referenced to V_{S-} , as in single-supply operation, then the total drive power is $V_S \times I_{OUT}$.

If the rms signal levels are indeterminate, then consider the worst case, when $V_{OUT} = V_S/4$ for R_L to midsupply.

$$P_D = (V_S \times I_S) + \frac{(V_S/4)^2}{R_L}$$

In single-supply operation with R_L referenced to V_{S-} , worst case is $V_{OUT} = V_S/2$.

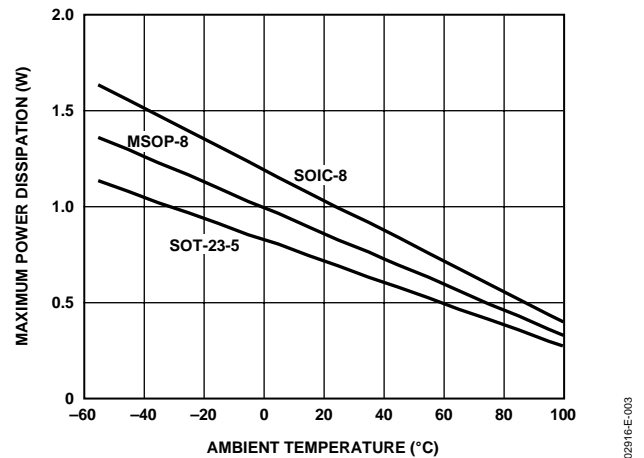


Figure 3. Maximum Power Dissipation vs. Temperature for a 4-Layer Board

Airflow will increase heat dissipation, effectively reducing θ_{JA} . Also, more metal directly in contact with the package leads from metal traces, through holes, ground, and power planes will reduce the θ_{JA} . Care must be taken to minimize parasitic capacitances at the input leads of high speed op amps as discussed in the Layout, Grounding, and Bypassing Considerations section.

Figure 3 shows the maximum safe power dissipation in the package versus the ambient temperature for the SOIC (125°C/W), SOT-23 (180°C/W), and MSOP (150°C/W) packages on a JEDEC standard 4-layer board. θ_{JA} values are approximations.

OUTPUT SHORT CIRCUIT

Shorting the output to ground or drawing excessive current for the AD8065/AD8066 will likely cause catastrophic failure.

TYPICAL PERFORMANCE CHARACTERISTICS

Default Conditions: $\pm 5\text{ V}$, $C_L = 5\text{ pF}$, $R_L = 1\text{ k}\Omega$, $V_{OUT} = 2\text{ V p-p}$, Temperature = 25°C .

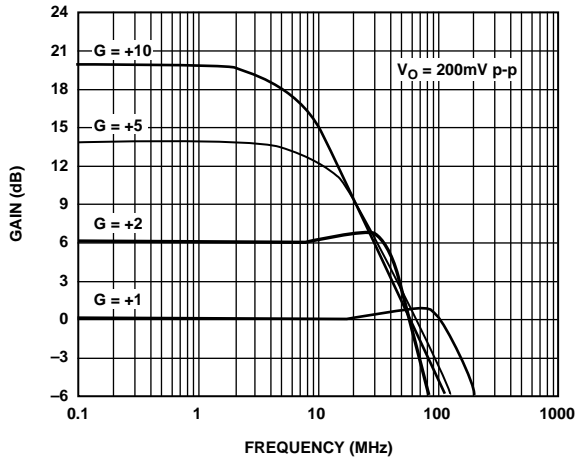


Figure 4. Small Signal Frequency Response for Various Gains

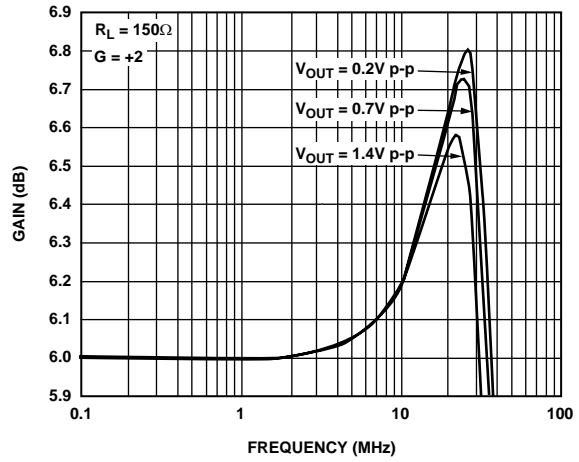


Figure 7. 0.1 dB Flatness Frequency Response (See Figure 43)

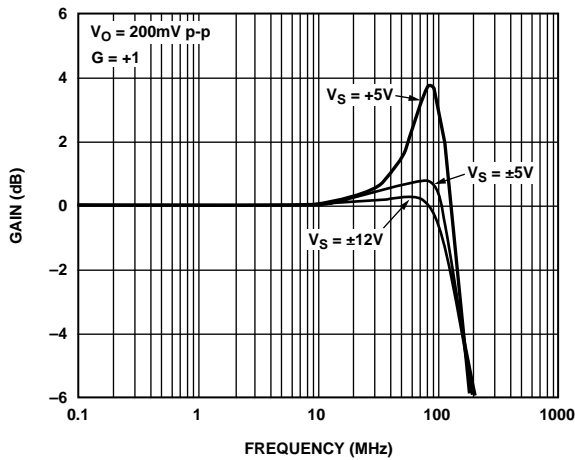


Figure 5. Small Signal Frequency Response for Various Supplies (See Figure 42)

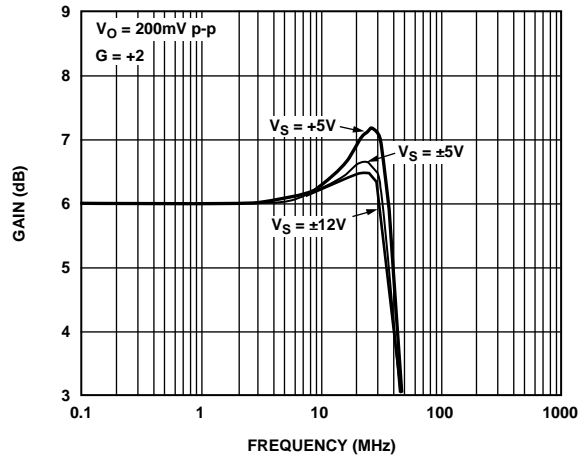


Figure 8. Small Signal Frequency Response for Various Supplies (See Figure 43)

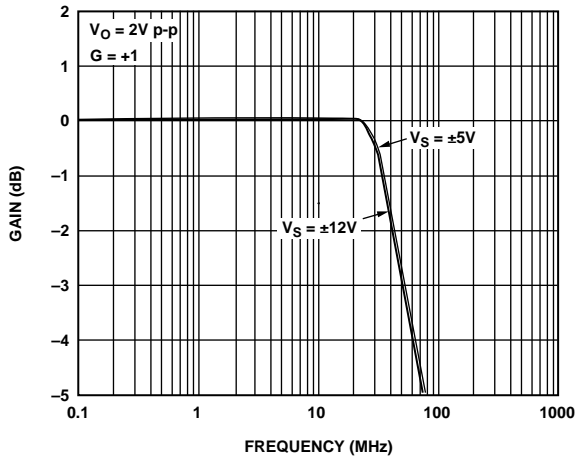


Figure 6. Large Signal Frequency Response for Various Supplies (See Figure 42)

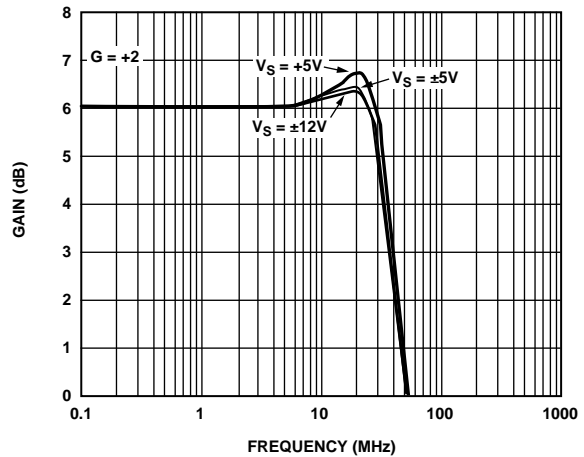
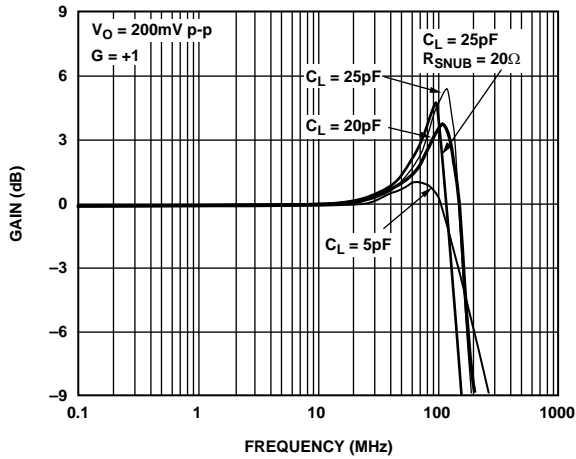
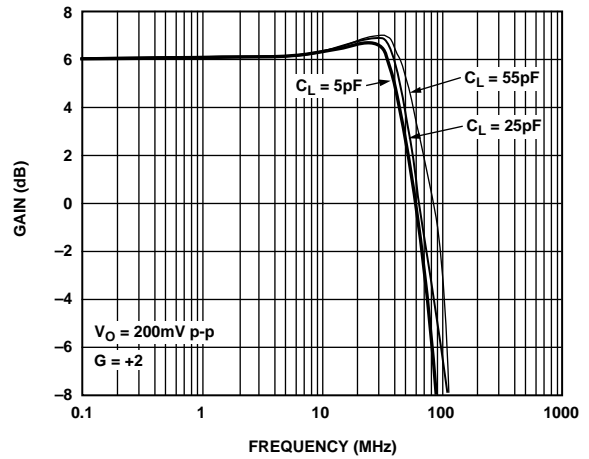


Figure 9. Large Signal Frequency Response for Various Supplies (See Figure 43)



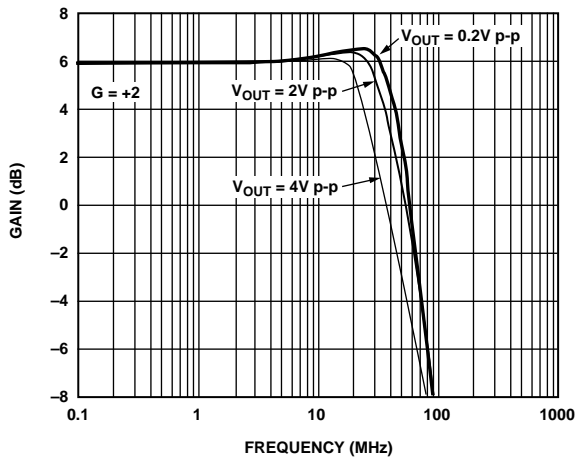
02916-E-010

Figure 10. Small Signal Frequency Response for Various C_{LOAD} (See Figure 42)



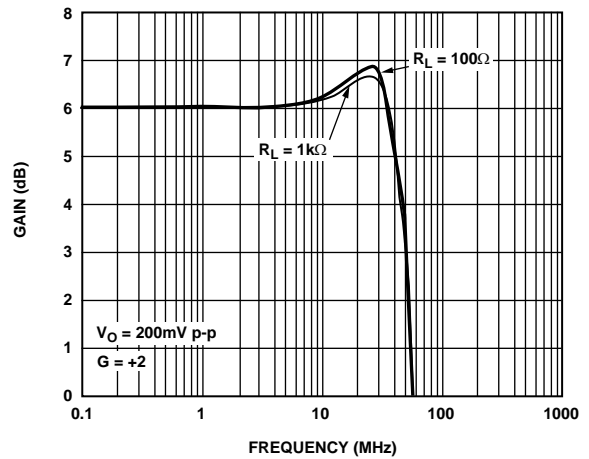
02916-E-013

Figure 13. Small Signal Frequency Response for Various C_{LOAD} (See Figure 43)



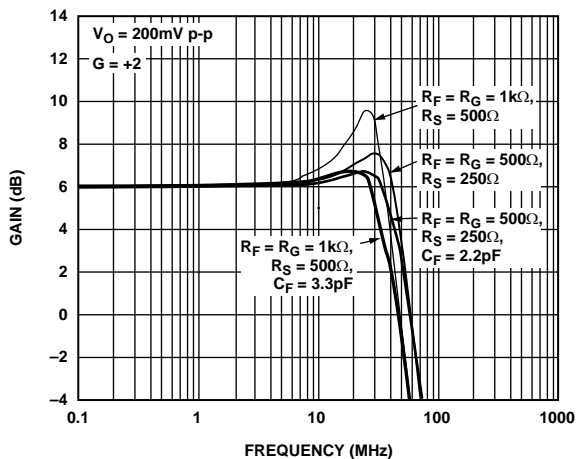
02916-E-011

Figure 11. Frequency Response for Various Output Amplitudes (See Figure 43)



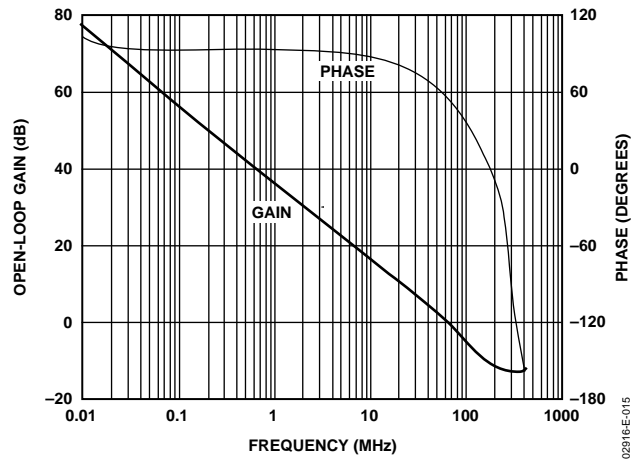
02916-E-014

Figure 14. Small Signal Frequency Response for Various R_{LOAD} (See Figure 43)



02916-E-012

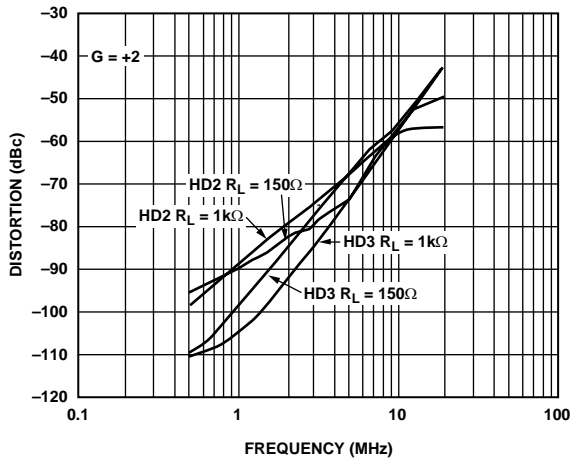
Figure 12. Small Signal Frequency Response for Various R_F/C_F (See Figure 43)



02916-E-015

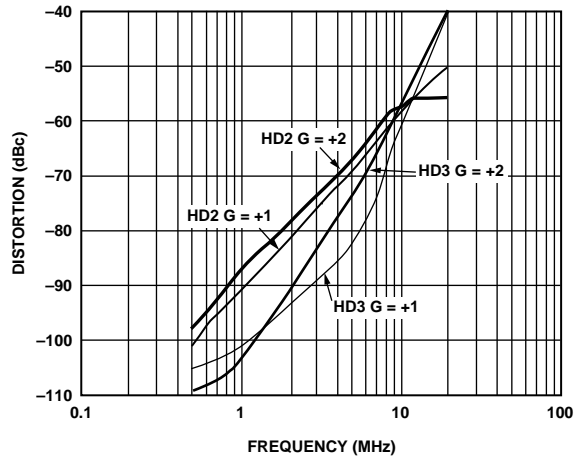
Figure 15. Open-Loop Response

AD8065/AD8066



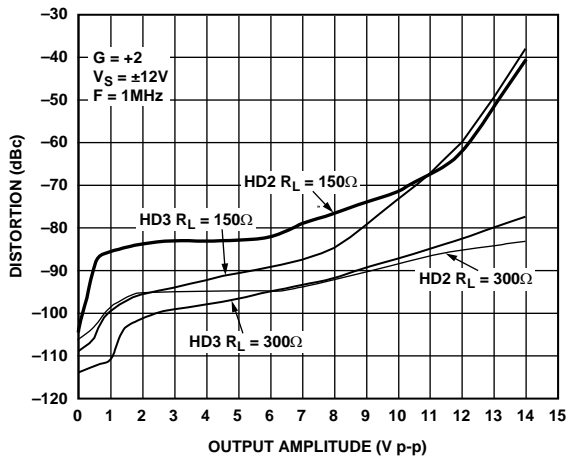
02916-E-016

Figure 16. Harmonic Distortion vs. Frequency for Various Loads (See Figure 43)



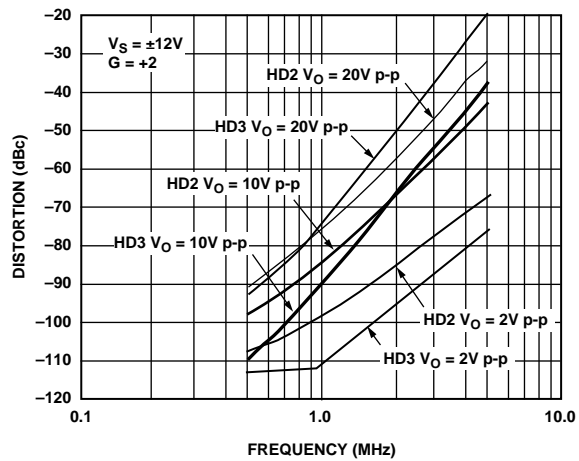
02916-E-019

Figure 19. Harmonic Distortion vs. Frequency for Various Gains (See Figure 42 and Figure 43)



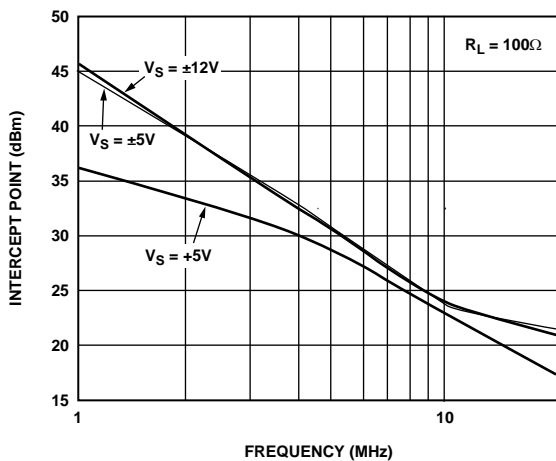
02916-E-017

Figure 17. Harmonic Distortion vs. Amplitude for Various Loads $V_S = \pm 12V$ (See Figure 43)



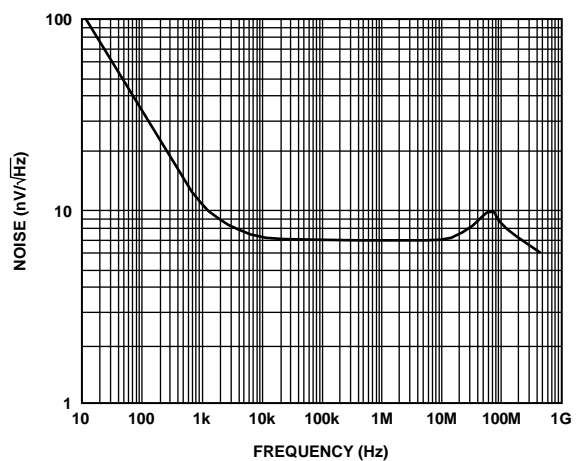
02916-E-020

Figure 20. Harmonic Distortion vs. Frequency for Various Amplitudes (See Figure 42 and Figure 43)



02916-E-018

Figure 18. Third-Order Intercept vs. Frequency and Supply Voltage



02916-E-021

Figure 21. Voltage Noise

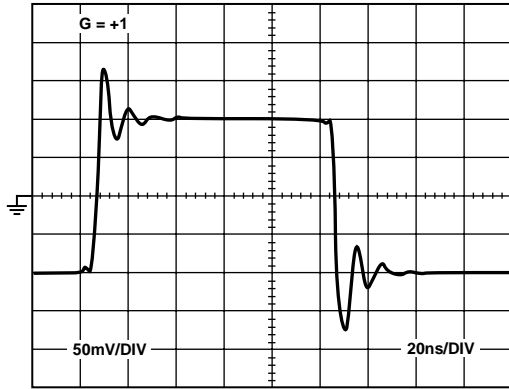


Figure 22. Small Signal Transient Response 5 V Supply (See Figure 52)

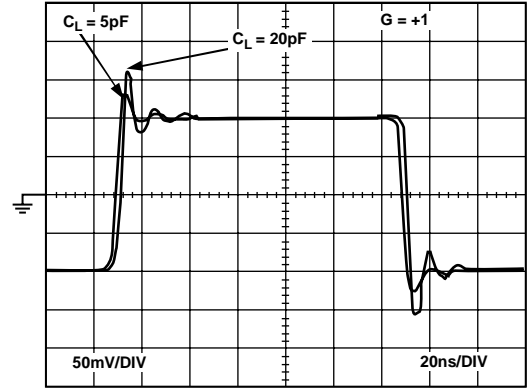


Figure 25. Small Signal Transient Response ±5 V (See Figure 42)

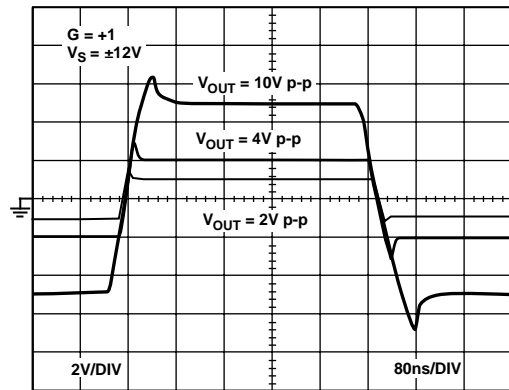


Figure 23. Large Signal Transient Response (See Figure 42)

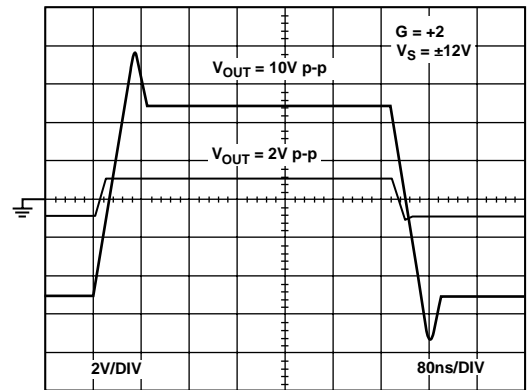


Figure 26. Large Signal Transient Response (See Figure 43)

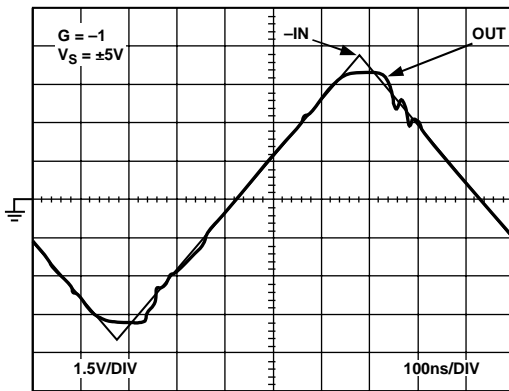


Figure 24. Output Overdrive Recovery (See Figure 44)

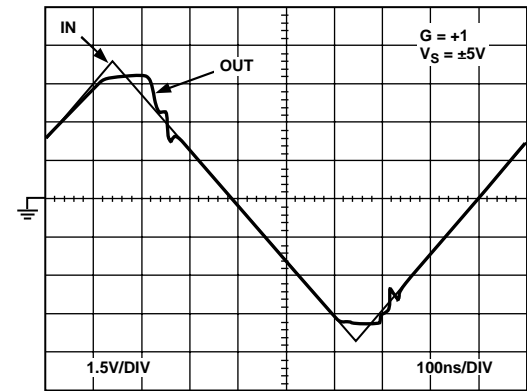


Figure 27. Input Overdrive Recovery (See Figure 42)

02916-E-022

02916-E-025

02916-E-023

02916-E-026

02916-E-024

02916-E-027

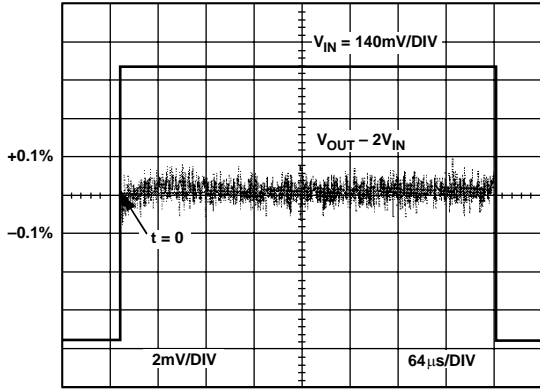


Figure 28. Long-Term Settling Time (See Figure 49)

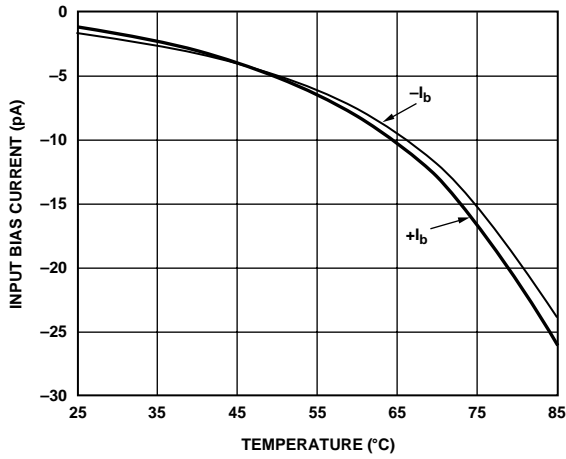


Figure 29. Input Bias Current vs. Temperature

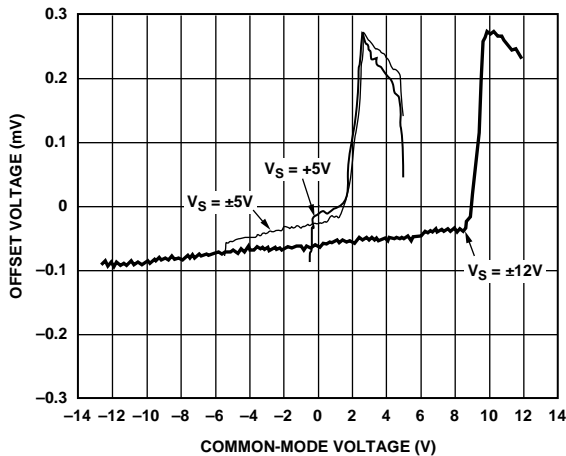


Figure 30. Input Offset Voltage vs. Common-Mode Voltage

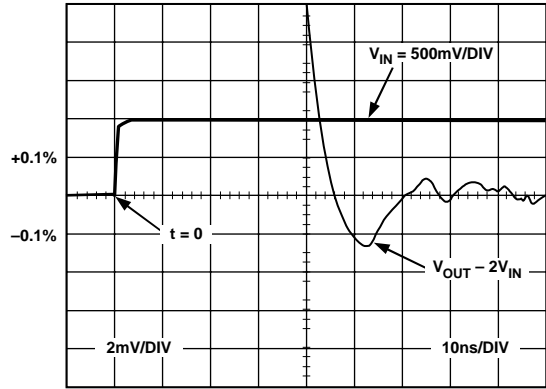


Figure 31. 0.1% Short-Term Settling Time (See Figure 49)

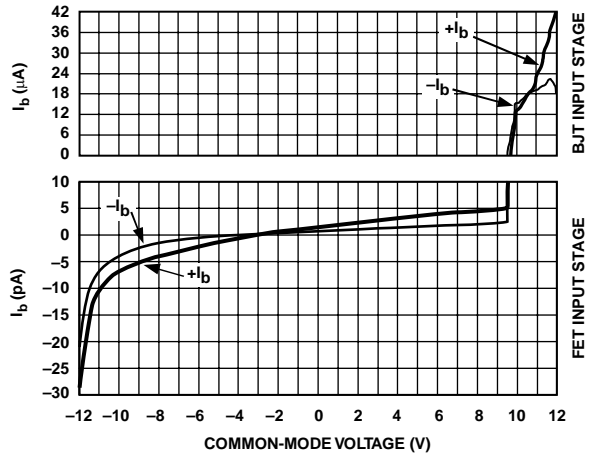


Figure 32. Input Bias Current vs. Common-Mode Voltage Range (see the Input and Output Overload Behavior section)

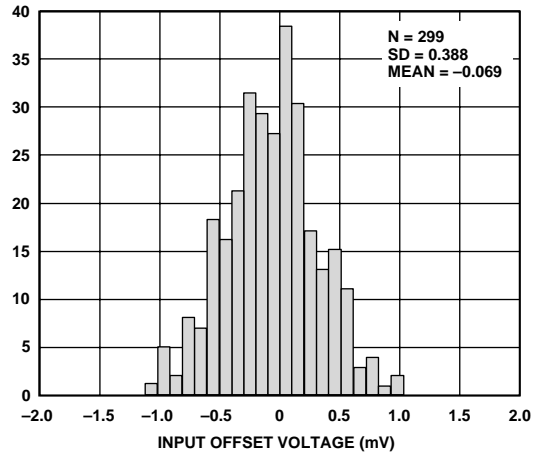


Figure 33. Input Offset Voltage

02916-E-028

02916-E-031

02916-E-029

02916-E-032

02916-E-030

02916-E-033

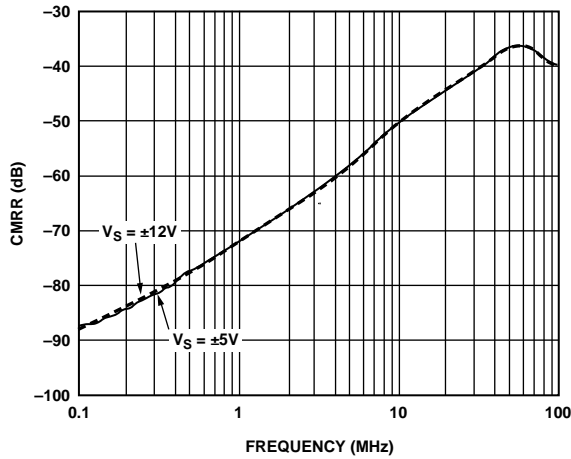


Figure 34. CMRR vs. Frequency (See Figure 46)

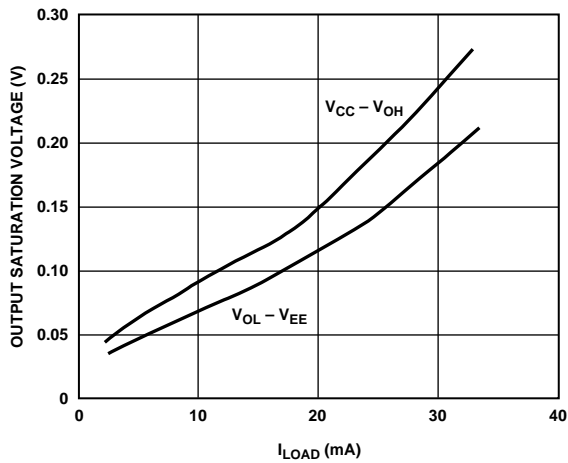


Figure 35. Output Saturation Voltage vs. Output Load Current

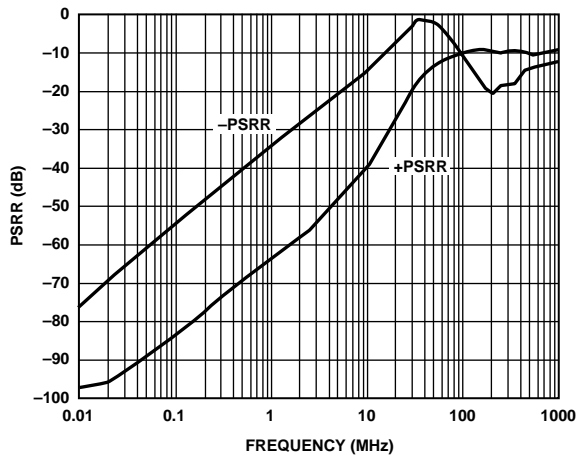


Figure 36. PSRR vs. Frequency (See Figure 48 and Figure 50)

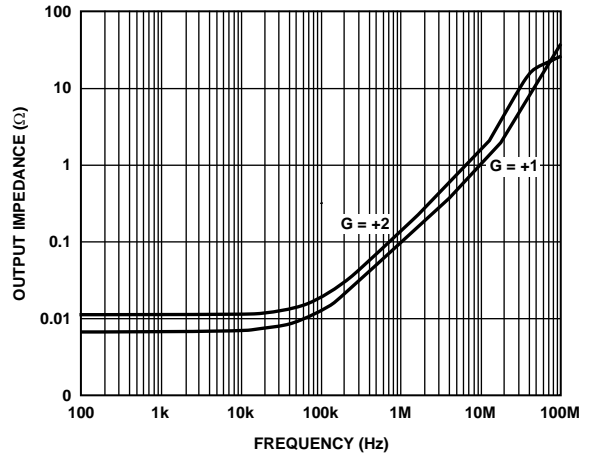


Figure 37. Output Impedance vs. Frequency (See Figure 45 and Figure 47)

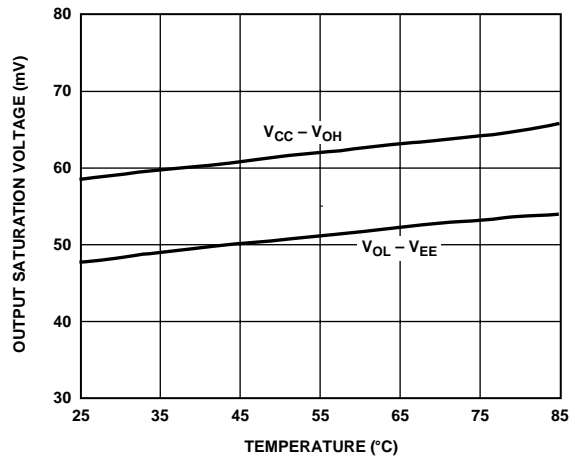


Figure 38. Output Saturation Voltage vs. Temperature

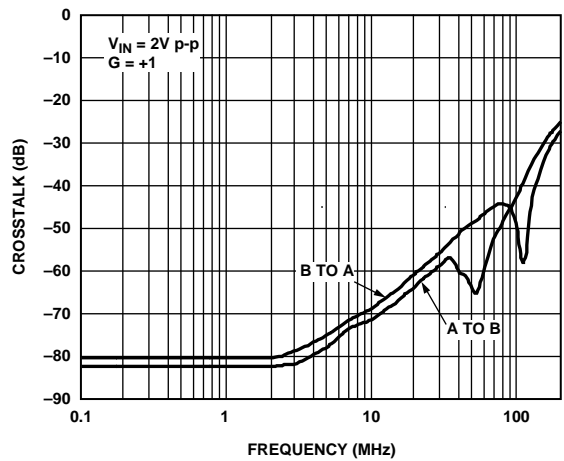


Figure 39. Crosstalk vs. Frequency (See Figure 51)

02916-E-084

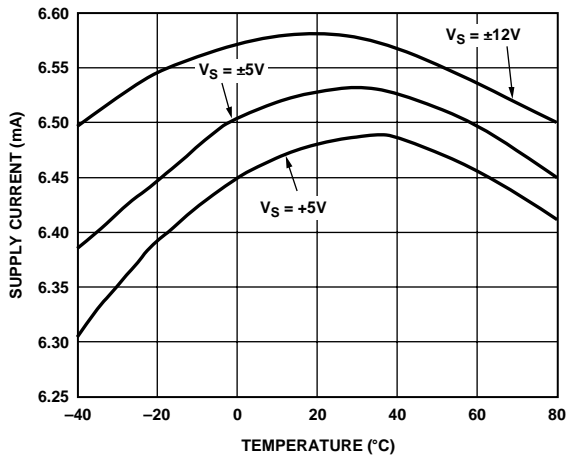
02916-E-087

02916-E-085

02916-E-038

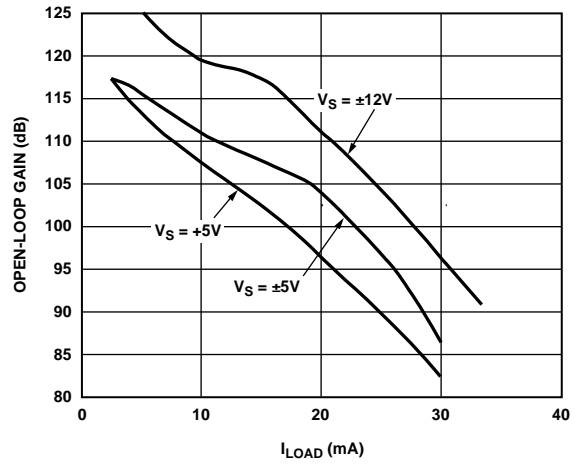
02916-E-086

02916-E-039



02916-E-040

Figure 40. Quiescent Supply Current vs. Temperature for Various Supply Voltages



02916-E-041

Figure 41. Open-Loop Gain vs. Load Current for Various Supply Voltages

TEST CIRCUITS

SOIC-8 Pinout

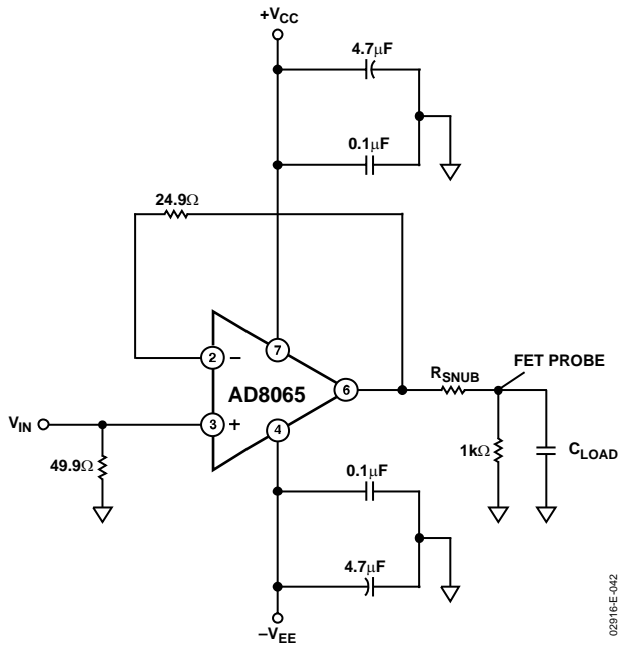


Figure 42. $G = +1$

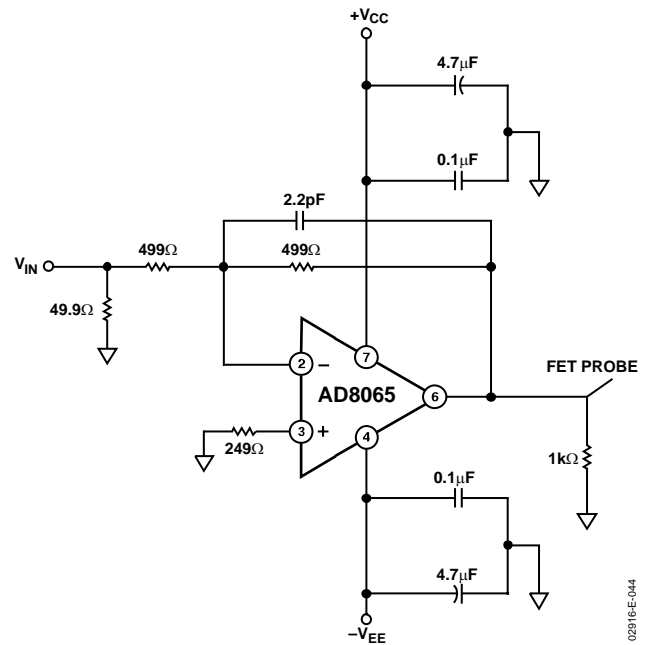


Figure 44. $G = -1$

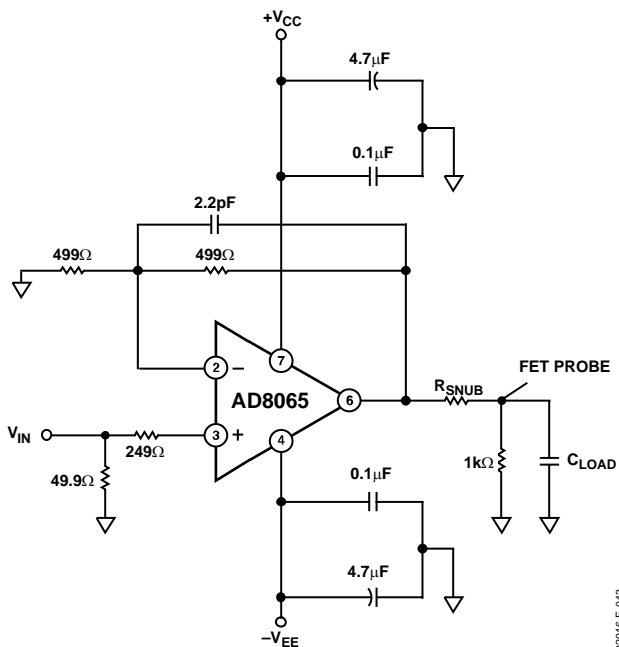


Figure 43. $G = +2$

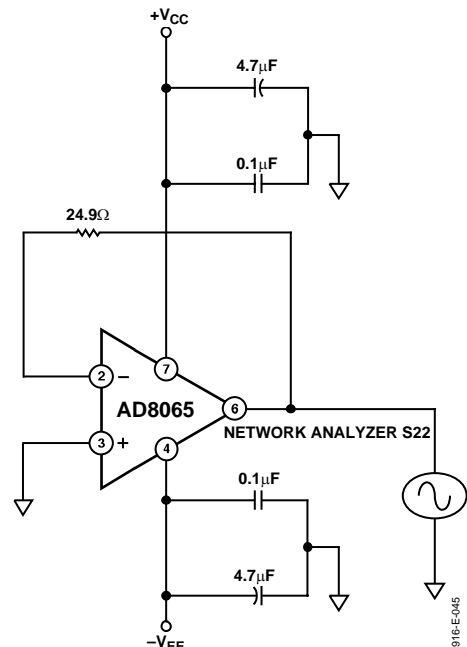


Figure 45. Output Impedance $G = +1$

AD8065/AD8066

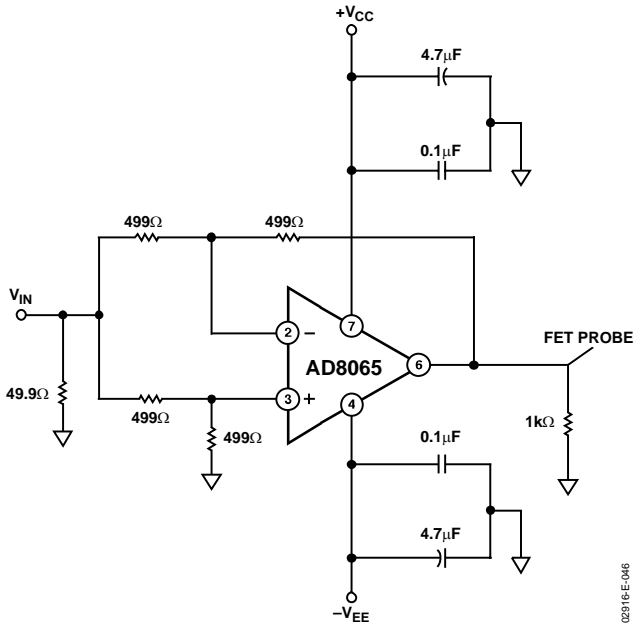


Figure 46. CMRR

02916-E-046

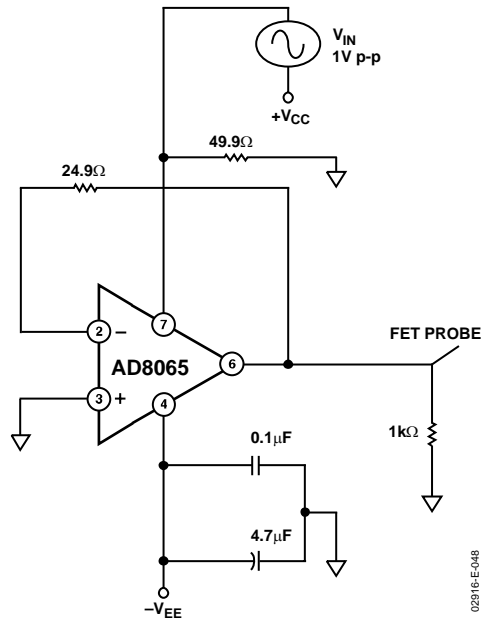


Figure 48. Positive PSRR

02916-E-048

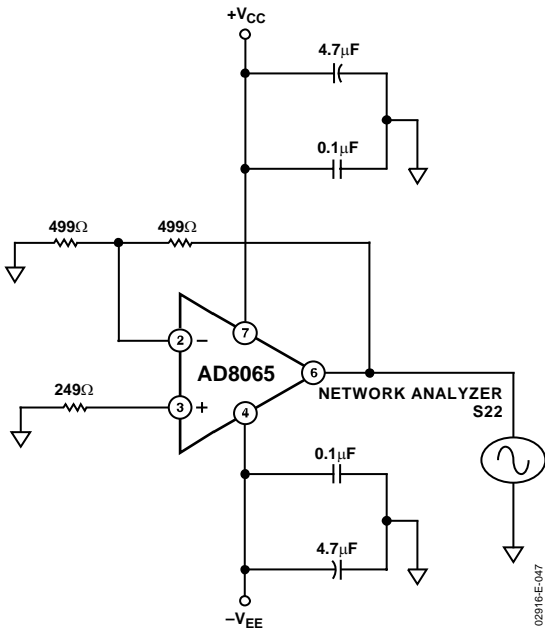


Figure 47. Output Impedance $G = +2$

02916-E-047

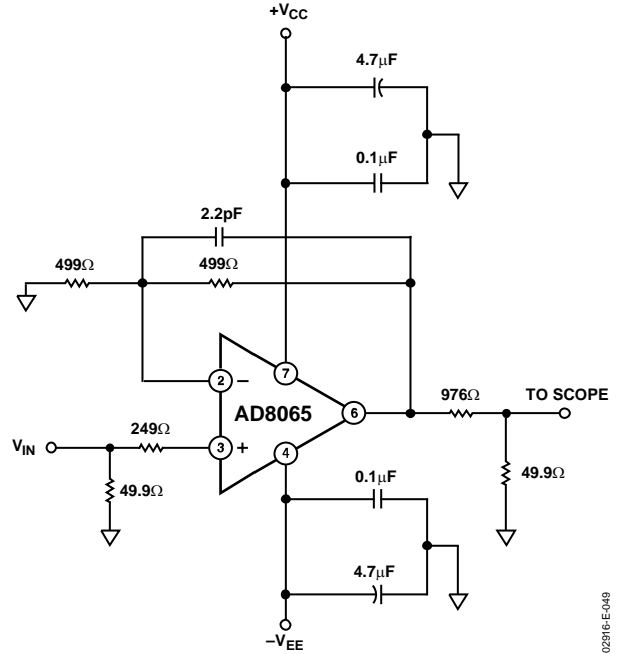


Figure 49. Settling Time

02916-E-049

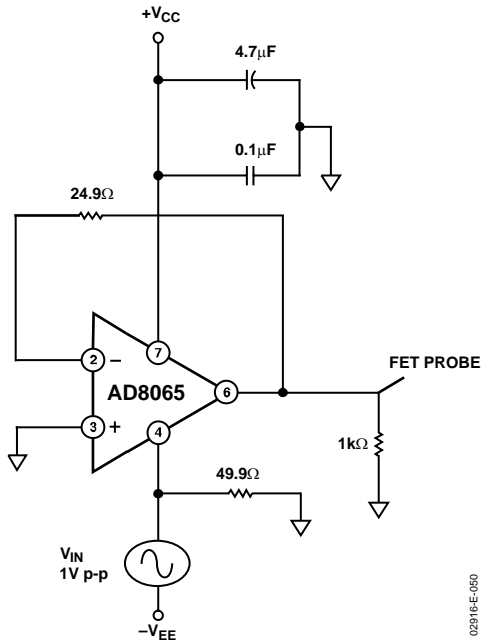


Figure 50. Negative PSRR

02916-E-050

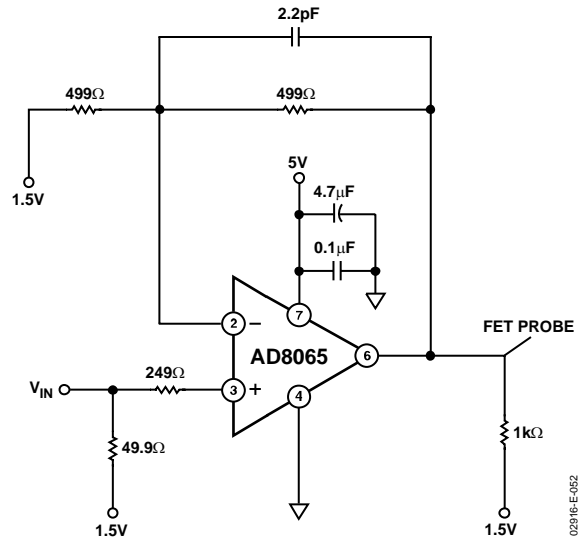


Figure 52. Single Supply

02916-E-052

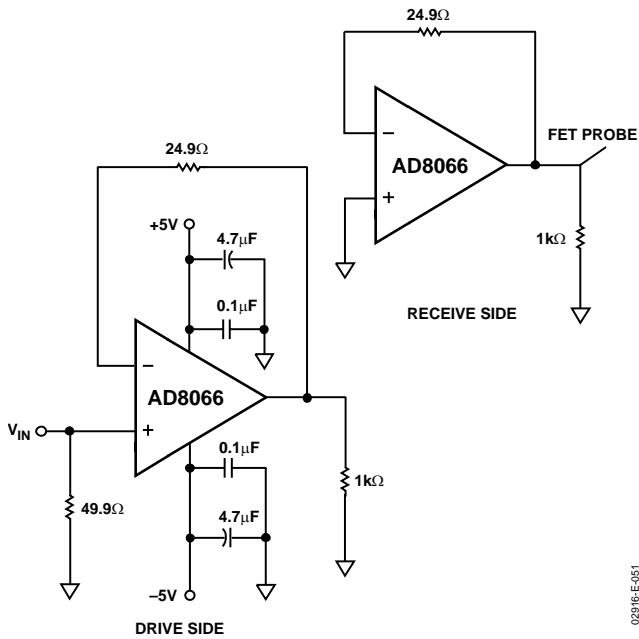


Figure 51. Crosstalk—AD8066

02916-E-051

THEORY OF OPERATION

The AD8065/AD8066 are voltage feedback operational amplifiers that combine a laser-trimmed JFET input stage with the Analog Devices eXtra Fast Complementary Bipolar (XFCB) process, resulting in an outstanding combination of precision and speed. The supply voltage range is from 5 V to 24 V. The amplifiers feature a patented rail-to-rail output stage capable of driving within 0.5 V of either power supply while sourcing or sinking up to 30 mA. Also featured is a single-supply input stage that handles common-mode signals from below the negative supply to within 3 V of the positive rail. Operation beyond the JFET input range is possible because of an auxiliary bipolar input stage that functions with input voltages up to the positive supply. The amplifiers operate as if they have a rail-to-rail input and exhibit no phase reversal behavior for common-mode voltages within the power supply.

With voltage noise of 7 nV/√Hz and -88 dBc distortion for 1 MHz 2 V p-p signals, the AD8065/AD8066 are a great choice for high resolution data acquisition systems. Their low noise, sub-pA input current, precision offset, and high speed make them superb preamps for fast photodiode applications. The speed and output drive capability of the AD8065/AD8066 also make them useful in video applications.

CLOSED-LOOP FREQUENCY RESPONSE

The AD8065/AD8066 are classic voltage feedback amplifiers with an open-loop frequency response that can be approximated as the integrator response shown in Figure 53. Basic closed-loop frequency response for inverting and noninverting configurations can be derived from the schematics shown.

NONINVERTING CLOSED-LOOP FREQUENCY RESPONSE

Solving for the transfer function

$$\frac{V_O}{V_I} = \frac{2\pi \times f_{crossover} (R_G + R_F)}{(R_F + R_G)s + 2\pi \times f_{crossover} \times R_G}$$

where $f_{crossover}$ is the frequency where the amplifier's open-loop gain equals 0 db

At dc $\frac{V_O}{V_I} = \frac{R_F + R_G}{R_G}$

Closed-loop -3 dB frequency

$$f_{-3dB} = f_{crossover} \times \frac{R_G}{R_F + R_G}$$

INVERTING CLOSED-LOOP FREQUENCY RESPONSE

$$\frac{V_O}{V_I} = \frac{-2\pi \times f_{crossover} \times R_F}{s(R_F + R_G) + 2\pi \times f_{crossover} \times R_G}$$

At dc $\frac{V_O}{V_I} = -\frac{R_F}{R_G}$

Closed-loop -3 dB frequency

$$f_{-3dB} = f_{crossover} \times \frac{R_G}{R_F + R_G}$$

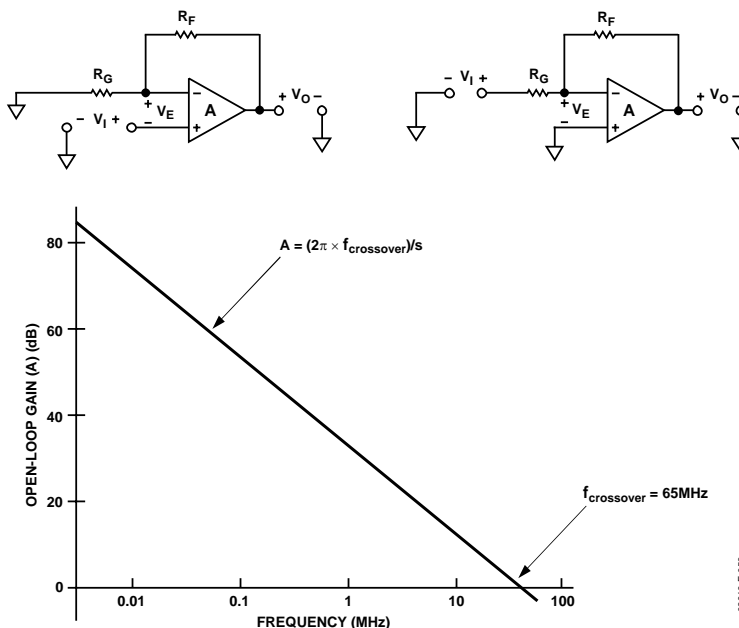


Figure 53. Open-Loop Gain vs. Frequency and Basic Connections

The closed-loop bandwidth is inversely proportional to the noise gain of the op amp circuit, $(R_F + R_G)/R_G$. This simple model is accurate for noise gains above 2. The actual bandwidth of circuits with noise gains at or below 2 will be higher than those predicted with this model due to the influence of other poles in the frequency response of the real op amp.

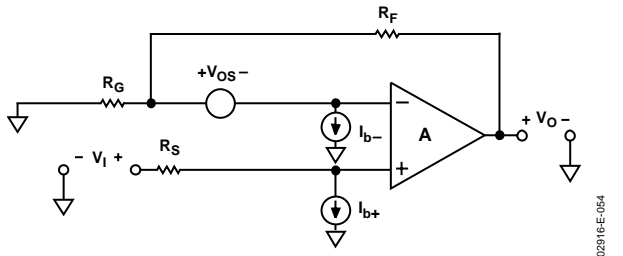


Figure 54. Voltage Feedback Amplifier DC Errors

Figure 54 shows a voltage feedback amplifier’s dc errors. For both inverting and noninverting configurations

$$V_O (error) = I_{b+} \times R_S \left(\frac{R_G + R_F}{R_G} \right) - I_{b-} \times R_F + V_{OS} \left(\frac{R_G + R_F}{R_G} \right)$$

The voltage error due to I_{b+} and I_{b-} is minimized if $R_S = R_F \parallel R_G$ (though with the AD8065 input currents at less than 20 pA over temperature, this is likely not a concern). To include common-mode and power supply rejection effects, total V_{OS} can be modeled as

$$V_{OS} = V_{OS_{nom}} + \frac{\Delta V_S}{PSR} + \frac{\Delta V_{CM}}{CMR}$$

$V_{OS_{nom}}$ is the offset voltage specified at nominal conditions, ΔV_S is the change in power supply from nominal conditions, PSR is the power supply rejection, ΔV_{CM} is the change in common-mode voltage from nominal conditions, and CMR is the common-mode rejection.

WIDEBAND OPERATION

Figure 42 through Figure 44 show the circuits used for wideband characterization for gains of +1, +2, and -1. Source impedance at the summing junction ($R_F \parallel R_G$) will form a pole in the amplifier’s loop response with the amplifier’s input capacitance of 6.6 pF. This can cause peaking and ringing if the time constant formed is too low. Feedback resistances of 300 Ω to 1 k Ω are recommended, since they will not unduly load down the amplifier and the time constant formed will not be too low. Peaking in the frequency response can be compensated for with a small capacitor (C_F) in parallel with the feedback resistor, as illustrated in Figure 12. This shows the effect of different feedback capacitances on the peaking and bandwidth for a noninverting $G = +2$ amplifier.

For the best settling times and the best distortion, the impedances at the AD8065/AD8066 input terminals should be matched. This minimizes nonlinear common-mode capacitive effects that can degrade ac performance.

Actual distortion performance depends on a number of variables:

- The closed-loop gain of the application
- Whether it is inverting or noninverting
- Amplifier loading
- Signal frequency and amplitude
- Board layout

Also see Figure 16 to Figure 20. The lowest distortion will be obtained with the AD8065 used in low gain inverting applications, since this eliminates common-mode effects. Higher closed-loop gains result in worse distortion performance.

INPUT PROTECTION

The inputs of the AD8065/AD8066 are protected with back-to-back diodes between the input terminals as well as ESD diodes to either power supply. This results in an input stage with picoamps of input current that can withstand up to 1500 V ESD events (human body model) with no degradation.

Excessive power dissipation through the protection devices will destroy or degrade the performance of the amplifier. Differential voltages greater than 0.7 V will result in an input current of approximately $(|V_+ - V_-| - 0.7 \text{ V})/R_I$, where R_I is the resistance in series with the inputs. For input voltages beyond the positive supply, the input current will be approximately $(V_I - V_{CC} - 0.7)/R_I$. Beyond the negative supply, the input current will be about $(V_I - V_{EE} + 0.7)/R_I$. If the inputs of the amplifier are to be subjected to sustained differential voltages greater than 0.7 V or to input voltages beyond the amplifier power supply, input current should be limited to 30 mA by an appropriately sized input resistor (R_I) as shown in Figure 55.

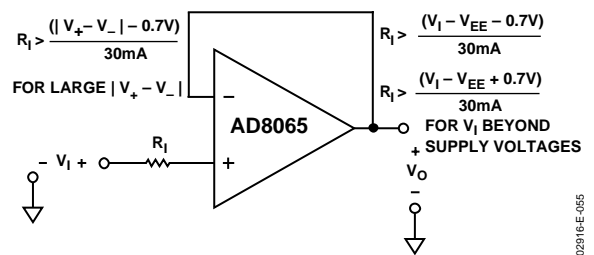


Figure 55. Current Limiting Resistor

THERMAL CONSIDERATIONS

With 24 V power supplies and 6.5 mA quiescent current, the AD8065 dissipates 156 mW with no load. The AD8066 dissipates 312 mW. This can lead to noticeable thermal effects, especially in the small SOT-23-5 (thermal resistance of 160°C/W). V_{OS} temperature drift is trimmed to guarantee a maximum drift of 17 $\mu\text{V}/^\circ\text{C}$, so it can change up to 0.425 mV due to warm-up effects for an AD8065/AD8066 in a SOT-23-5 package on 24 V.

I_b increases by a factor of 1.7 for every 10°C rise in temperature. I_b will be close to 5 times higher at 24 V supplies as opposed to a single 5 V supply.

Heavy loads will increase power dissipation and raise the chip junction temperature as described in the Maximum Power Dissipation section. Care should be taken to not exceed the rated power dissipation of the package.

INPUT AND OUTPUT OVERLOAD BEHAVIOR

The AD8065/AD8066 have internal circuitry to guard against phase reversal due to overdriving the input stage. A simplified schematic of the input stage, including the input-protection diodes and antiphase reversal circuitry, is shown in Figure 56.

The circuit is arranged such that when the input common-mode voltage exceeds a certain threshold, the input JFET pair's bias current will turn OFF, and the bias current of an auxiliary NPN pair will turn ON, taking over control of the amplifier. When the input common-mode voltage returns to a viable operating value, the FET stage turns back ON, the NPN stage turns OFF, and normal operation resumes.

The NPN pair can sustain operation with the input voltage up to the positive supply, so this is a pseudo rail-to-rail input stage. For operation beyond the FET stage's common-mode limit, the amplifier's V_{OS} will change to the NPN pair's offset (mean of 160 μV , standard deviation of 820 μV), and I_b will increase to the NPN pair's base current up to 45 μA (see Figure 32).

Switchback, or recovery time, is about 100 ns, see Figure 27.

The output transistors of the rail-to-rail output stage have circuitry to limit the extent of their saturation when the output is overdriven. This helps output recovery time. Output recovery from a 0.5 V output overdrive on a ± 5 V supply is shown in Figure 24.

LAYOUT, GROUNDING, AND BYPASSING CONSIDERATIONS

POWER SUPPLY BYPASSING

Power supply pins are actually inputs and care must be taken so that a noise-free stable dc voltage is applied. The purpose of bypass capacitors is to create low impedances from the supply to ground at all frequencies, thereby shunting or filtering most of the noise.

Decoupling schemes are designed to minimize the bypassing impedance at all frequencies with a parallel combination of capacitors. 0.1 μF (X7R or NPO) chip capacitors are critical and should be as close as possible to the amplifier package. The 4.7 μF tantalum capacitor is less critical for high frequency bypassing, and, in most cases, only one is needed per board, at the supply inputs.

GROUNDING

A ground plane layer is important in densely packed PC boards to spread the current minimizing parasitic inductances. However, an understanding of where the current flows in a circuit is critical to implementing effective high speed circuit design. The length of the current path is directly proportional to the magnitude of parasitic inductances and therefore the high frequency impedance of the path. High speed currents in an inductive ground return will create an unwanted voltage noise.

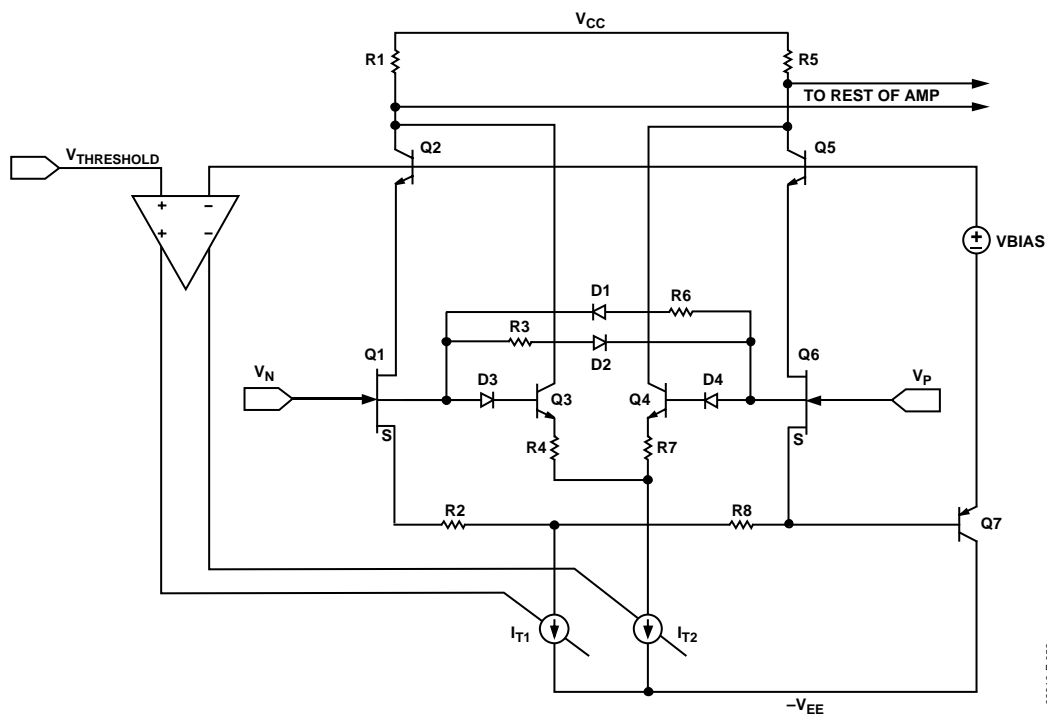


Figure 56. Simplified Input Stage

02816-E-056

The length of the high frequency bypass capacitor leads is most critical. A parasitic inductance in the bypass grounding will work against the low impedance created by the bypass capacitor. Place the ground leads of the bypass capacitors at the same physical location. Because load currents flow from the supplies as well, the ground for the load impedance should be at the same physical location as the bypass capacitor grounds. For the larger value capacitors, which are effective at lower frequencies, the current return path distance is less critical.

LEAKAGE CURRENTS

Poor PC board layout, contaminants, and the board insulator material can create leakage currents that are much larger than the input bias current of the AD8065/AD8066. Any voltage differential between the inputs and nearby runs will set up leakage currents through the PC board insulator, for example, $1\text{ V}/100\text{ G}\Omega = 10\text{ pA}$. Similarly, any contaminants on the board can create significant leakage (skin oils are a common problem). To significantly reduce leakage, put a guard ring (shield) around the inputs and input leads that are driven to the same voltage potential as the inputs. This way there is no voltage potential between the inputs and surrounding area to set up any leakage currents. For the guard ring to be completely effective, it must be driven by a relatively low impedance source and should completely surround the input leads on all sides, above and below, using a multilayer board.

Another effect that can cause leakage currents is the charge absorption of the insulator material itself. Minimizing the amount of material between the input leads and the guard ring will help to reduce the absorption. Also, low absorption materials, such as Teflon® or ceramic, could be necessary in some instances.

INPUT CAPACITANCE

Along with bypassing and ground, high speed amplifiers can be sensitive to parasitic capacitance between the inputs and ground. A few pF of capacitance will reduce the input impedance at high frequencies, in turn increasing the amplifier's gain, causing peaking of the frequency response or even oscillations, if severe enough. It is recommended that the external passive components connected to the input pins be placed as close as possible to the inputs to avoid parasitic capacitance. The ground and power planes must be kept at a small distance from the input pins on all layers of the board.

OUTPUT CAPACITANCE

To a lesser extent, parasitic capacitances on the output can cause peaking and ringing of the frequency response. There are two methods to effectively minimize their effect.

- As shown in Figure 57, put a small value resistor (R_S) in series with the output to isolate the load capacitor from the amp's output stage. A good value to choose is $20\ \Omega$ (see Figure 10).
- Increase the phase margin with higher noise gains or add a pole with a parallel resistor and capacitor from $-IN$ to the output.

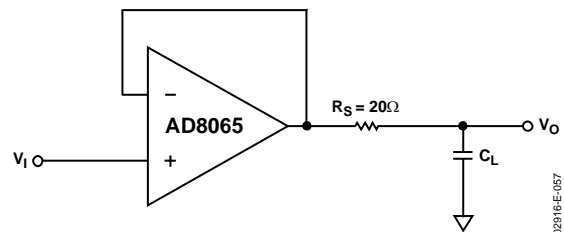


Figure 57. Output Isolation Resistor

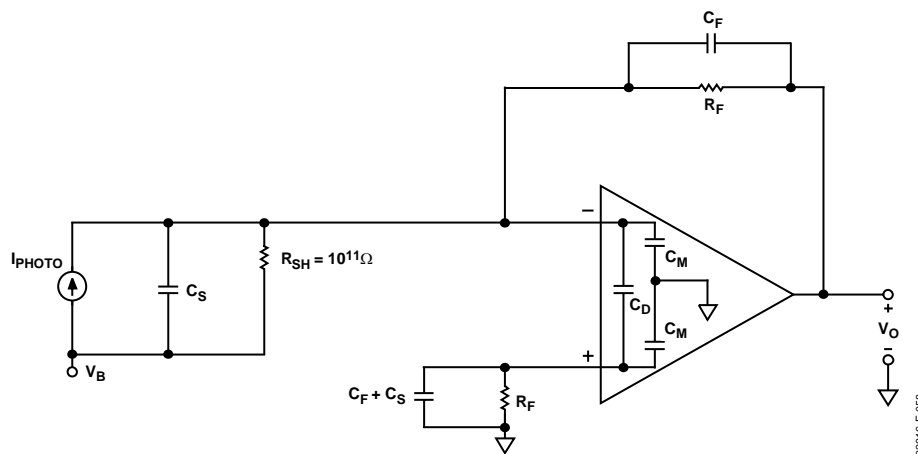


Figure 58. Wideband Photodiode Preamp

INPUT-TO-OUTPUT COUPLING

In order to minimize capacitive coupling between the inputs and output, the output signal traces should not be parallel with the inputs.

WIDEBAND PHOTODIODE PREAMP

Figure 58 shows an I/V converter with an electrical model of a photodiode. The basic transfer function is where

$$V_{OUT} = \frac{I_{PHOTO} \times R_F}{1 + sC_F R_F}$$

where I_{PHOTO} is the output current of the photodiode, and the parallel combination of R_F and C_F set the signal bandwidth.

The stable bandwidth attainable with this preamp is a function of R_F , the gain bandwidth product of the amplifier, and the total capacitance at the amplifier's summing junction, including C_S and the amplifier input capacitance. R_F and the total capacitance produce a pole in the amplifier's loop transmission that can result in peaking and instability. Adding C_F creates a 0 in the loop transmission, which compensates for the pole's effect and reduces the signal bandwidth. It can be shown that the signal bandwidth resulting in a 45° phase margin ($f_{(45)}$) is defined by the expression

$$f_{(45)} = \sqrt{\frac{f_{CR}}{2\pi \times R_F \times C_S}}$$

where f_{CR} is the amplifier crossover frequency, R_F is the feedback resistor, and C_S is the total capacitance at the amplifier summing junction (amplifier + photodiode + board parasitics).

The value of C_F that produces $f_{(45)}$ can be shown to be

$$C_F = \sqrt{\frac{C_S}{2\pi \times R_F \times f_{CR}}}$$

The frequency response in this case will show about 2 dB of peaking and 15% overshoot. Doubling C_F and cutting the bandwidth in half will result in a flat frequency response, with about 5% transient overshoot.

Table 5. RMS Noise Contributions of Photodiode Preamp

Contributor	Expression	RMS Noise with $R_F = 50 \text{ k}\Omega$, $C_S = 15 \text{ pF}$, $C_F = 2 \text{ pF}$
R_F (x2)	$\sqrt{2 \times 4 kT \times R_F \times f_2 \times 1.57}$	64.5 μV
Amp to f_1	$VEN \times \sqrt{f_1}$	2.4 μV
Amp ($f_2 - f_1$)	$VEN \times \sqrt{\frac{C_S + C_M + C_F + 2C_D}{C_F}} \times \sqrt{f_2 - f_1}$	31 μV
Amp to (past f_2)	$VEN \times \sqrt{\frac{C_S + C_M + C_D + 2C_F}{C_F}} \times \sqrt{f_3 \times 1.57}$	260 μV

270 μV (Total)

The preamp's output noise over frequency is shown in Figure 59.

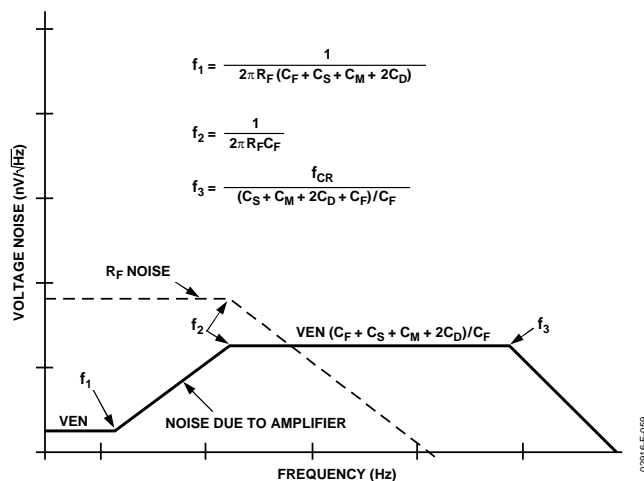


Figure 59. Photodiode Voltage Noise Contributions

The pole in the loop transmission translates to a 0 in the amplifier's noise gain, leading to an amplification of the input voltage noise over frequency. The loop transmission 0 introduced by C_F limits the amplification. The noise gain bandwidth extends past the preamp signal bandwidth and is eventually rolled off by the decreasing loop gain of the amplifier. Keeping the input terminal impedances matched is recommended to eliminate common-mode noise peaking effects, which will add to the output noise.

Integrating the square of the output voltage noise spectral density over frequency and then taking the square root allows users to obtain the total rms output noise of the preamp. Table 5 summarizes approximations for the amplifier and feedback and source resistances. Noise components for an example preamp with $R_F = 50 \text{ k}\Omega$, $C_S = 15 \text{ pF}$, and $C_F = 2 \text{ pF}$ (bandwidth of about 1.6 MHz) are also listed.

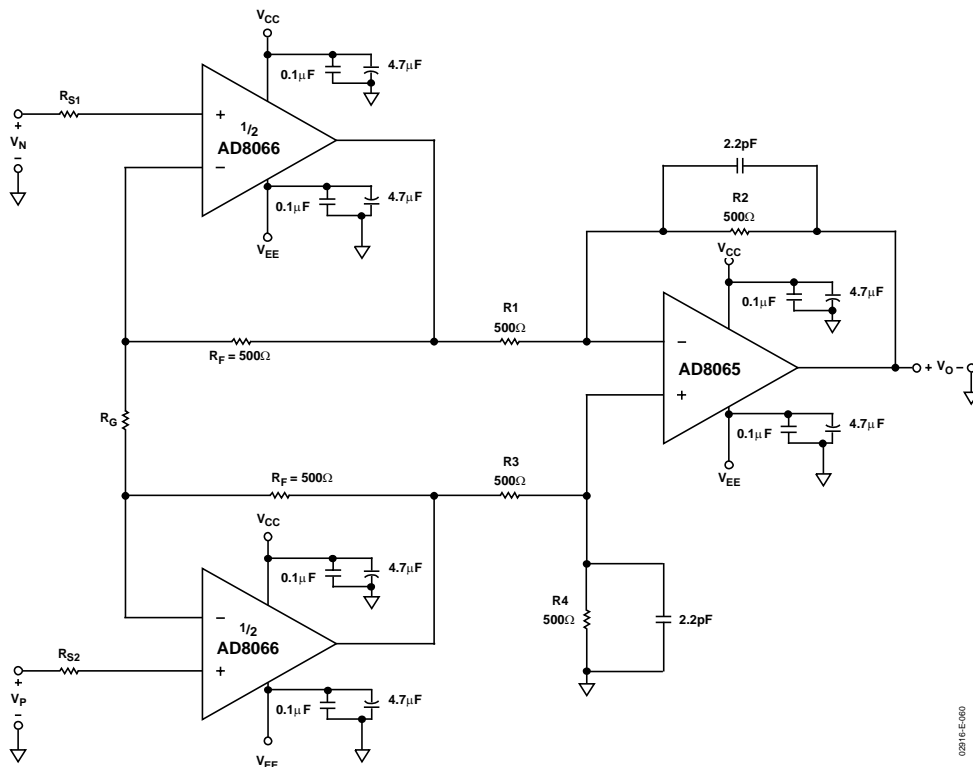


Figure 60. High Speed Instrumentation Amplifier

HIGH SPEED JFET INPUT INSTRUMENTATION AMPLIFIER

Figure 60 shows an example of a high speed instrumentation amplifier with high input impedance using the AD8065/AD8066. The dc transfer function is

$$V_{OUT} = (V_N - V_P) \left(\frac{1 + 1000}{R_G} \right)$$

For $G = +1$, it is recommended that the feedback resistors for the two preamps be set to a low value (for instance 50Ω for 50Ω source impedance). The bandwidth for $G = +1$ will be 50 MHz . For higher gains, the bandwidth will be set by the preamp, equaling

$$Inamp_{-3dB} = (f_{CR} \times R_G) / (2 \times R_F)$$

Common-mode rejection of the inamp will be primarily determined by the match of the resistor ratios $R1:R2$ to $R3:R4$. It can be estimated

$$\frac{V_O}{V_{CM}} = \frac{(\delta 1 - \delta 2)}{(1 + \delta 1) \delta 2}$$

The summing junction impedance for the preamps is equal to

$R_F \parallel 0.5(R_G)$. This is the value to be used for matching purposes.

VIDEO BUFFER

The output current capability and speed of the AD8065 make it useful as a video buffer, shown in Figure 61.

The $G = +2$ configuration compensates for the voltage division of the signal due to the signal termination. This buffer maintains 0.1 dB flatness for signals up to 7 MHz , from low amplitudes up to 2 V p-p (Figure 7). Differential gain and phase have been measured to be 0.02% and 0.028° at $\pm 5 \text{ V}$ supplies.

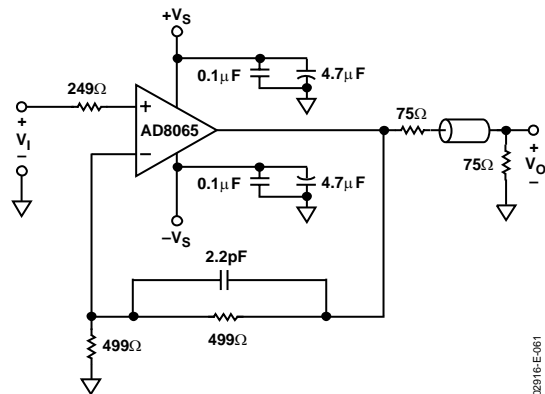
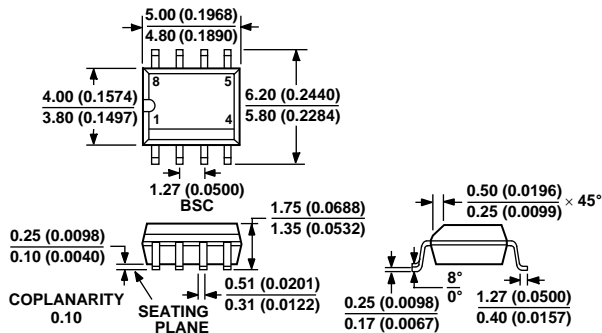


Figure 61. Video Buffer

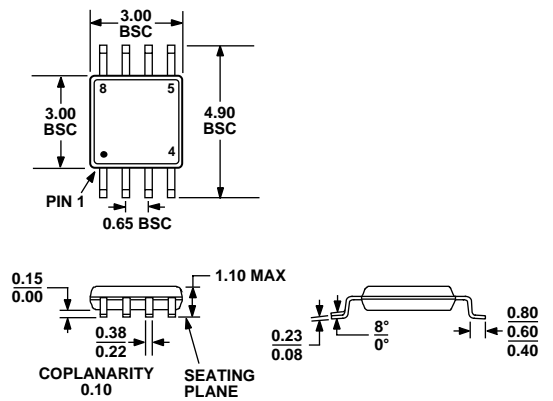
OUTLINE DIMENSIONS



COMPLIANT TO JEDEC STANDARDS MS-012AA
 CONTROLLING DIMENSIONS ARE IN MILLIMETERS; INCH DIMENSIONS
 (IN PARENTHESES) ARE ROUNDED-OFF MILLIMETER EQUIVALENTS FOR
 REFERENCE ONLY AND ARE NOT APPROPRIATE FOR USE IN DESIGN

Figure 62. 8-Lead Standard Small Outline Package Narrow Body [SOIC]
 (R-8)

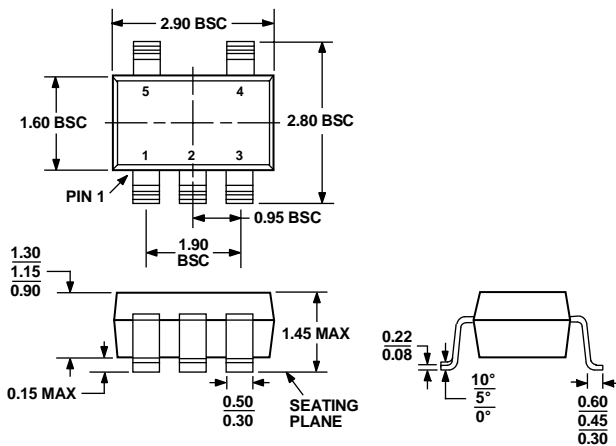
Dimensions shown in millimeters (inches)



COMPLIANT TO JEDEC STANDARDS MO-187AA

Figure 64. 8-Lead Mini Small Outline Package [MSOP]
 (RM-8)

Dimensions shown in millimeters



COMPLIANT TO JEDEC STANDARDS MO-178AA

Figure 63. 5-Lead Small Outline Transistor Package [SOT-23]
 (RT-5)

Dimensions shown in millimeters

AD8065/AD8066

ORDERING GUIDE

Model	Temperature Range	Package Description	Package Outline	Branding
AD8065AR	-40°C to +85°C	8-Lead SOIC	R-8	
AD8065AR-REEL	-40°C to +85°C	8-Lead SOIC	R-8	
AD8065AR-REEL7	-40°C to +85°C	8-Lead SOIC	R-8	
AD8065ART-REEL	-40°C to +85°C	5-Lead SOT-23	RT-5	HRA
AD8065ART-R2	-40°C to +85°C	5-Lead SOT-23	RT-5	HRA
AD8065ART-REEL7	-40°C to +85°C	5-Lead SOT-23	RT-5	HRA
AD8066AR	-40°C to +85°C	8-Lead SOIC	R-8	
AD8066AR-REEL	-40°C to +85°C	8-Lead SOIC	R-8	
AD8066AR-REEL7	-40°C to +85°C	8-Lead SOIC	R-8	
AD8066ARZ ¹	-40°C to +85°C	8-Lead SOIC	R-8	
AD8066ARZ-REEL ¹	-40°C to +85°C	8-Lead SOIC	R-8	
AD8066ARZ-REEL7 ¹	-40°C to +85°C	8-Lead SOIC	R-8	
AD8066ARM	-40°C to +85°C	8-Lead MSOP	RM-8	HIB
AD8066ARM-REEL	-40°C to +85°C	8-Lead MSOP	RM-8	HIB
AD8066ARM-REEL7	-40°C to +85°C	8-Lead MSOP	RM-8	HIB

¹ Z = Pb-free part.

NOTES

NOTES